

Sea Surface Reflectivity Variation With Ocean Temperature at Ka-Band Observed Using Near-Nadir Satellite Radar Data

Douglas Vandemark, *Senior Member, IEEE*, Bertrand Chapron, Hui Feng, and Alexis Mouche

Abstract—Satellite ocean radar data are used to assess the flat surface reflectivity for seawater at 36 GHz by comparison to an existing model for dielectric constant variation. Sea surface temperature (SST) is the dominant control, and results indicate a 14% variation in the normalized radar cross section (NRCS) at Ka-band (35.75 GHz) that is in close agreement with model prediction. Consistent results are obtained globally using near-nadir incidence data from both the SARAL AltiKa radar altimeter and Global Precipitation Measurement mission rain radar. The observations affirm that small but systematic SST-dependent corrections at Ka-band may require consideration prior to NRCS use in ocean surface wave investigations and applications. As an example, we demonstrate a systematic improvement in AltiKa ocean wind speed inversions after such an SST adjustment. Lower frequency C- and Ku-band results are also assessed to confirm the general agreement with prediction and a much smaller variation due to SST.

Index Terms—AltiKa, fresnel surface reflection, global precipitation measurement (GPM), ka-band, mean square slope, normalized radar cross section (NRCS), ocean altimetry, ocean backscatter, ocean emissivity, sea surface roughness, sea surface temperature (SST), specular reflectance, wind speed, 36 GHz.

I. INTRODUCTION

THE majority of the ocean observing satellite radar systems deployed to date operate at frequencies at or below 14 GHz (Ku-band), where the ocean radar backscatter is thought to vary little due to any change in the dielectric properties of seawater. In these cases, one typically neglects any variation in surface reflectance that is known to depend weakly on dielectric constant variation attributed to temperature and salinity change in the upper ocean. As one example, consider radar altimetry where the ocean normalized radar cross section (NRCS) σ_0 near nadir is well approximated using a quasi-optical model such as in [1]

$$\sigma_0(\theta) \cong \rho / \text{mss}_{\text{eff}} \cdot \sec^4 \theta \cdot \exp^{-\tan^2 \theta / \text{mss}_{\text{eff}}} \quad (1)$$

Manuscript received October 1, 2015; revised November 12, 2015; accepted January 19, 2016. This work was supported by the National Aeronautics and Space Administration under Grant NNX13AE17G.

D. Vandemark and H. Feng are with the Institute for the Study of Earth, Oceans, and Space, University of New Hampshire, Durham, NH 03824 USA (e-mail: doug.vandemark@unh.edu).

B. Chapron and A. Mouche are with the Institut Français de Recherche pour l'Exploitation de la Mer (IFREMER)/Centre de Bretagne, 29280 Plouzané, France.

Color versions of one or more of the figures in this paper are available online at <http://ieeexplore.ieee.org>.

Digital Object Identifier 10.1109/LGRS.2016.2520823

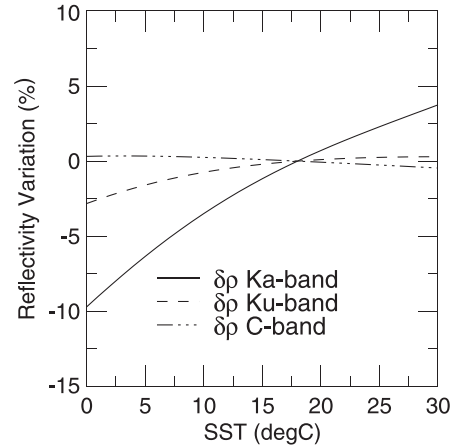


Fig. 1. Perturbation of ρ (in percent) with seawater temperature change as predicted by MW04 (solid line) at Ka-, Ku-, and C-band. In each case, the estimates are normalized by their value at SST = 18 °C.

where θ is the incidence angle with respect to nadir and mss_{eff} is the effective total ocean surface slope variance. The specular reflectivity ρ is derived from the nadir Fresnel reflection coefficient $R(0^\circ)$, with $\rho \equiv |R(0) * R(0)^*|$ and where R is a function of sea surface salinity, temperature, and frequency. For the case of a fixed sea surface roughness $\text{mss}_{\text{eff}} = \text{constant}$, any remaining variation in σ_0 is then carried in the reflectivity. Semiempirical seawater emission and reflectivity models at microwave frequencies [4]–[6] have been developed and refined to account for this variability, most often for use in microwave radiometer applications. For incidence angles near nadir and at L- to Ku-band (1–14 GHz), the full range of reflectivity variation due to sea surface temperature (SST) is at most 3% (highest at Ku-band). This is illustrated for C-, Ku-, and Ka-band in Fig. 1. Above L-band, any change due to ocean salinities ranging from 30 to 38 psu is more than a factor of ten less. Most satellite ocean radar backscatter applications are subject to geophysical variability and signal-to-noise concerns that significantly exceed these levels, and thus variation in reflectivity due to SST is typically neglected.

Recently, two new radar systems have been deployed in space operating at the higher Ka-band frequency (near 36 GHz), while several additional missions, including the Surface Water and Ocean Topography sensor [2], are in advanced planning stages. The two platforms now in orbit are AltiKa [3] and the Global Precipitation Measurement (GPM) dual-frequency

precipitation radar (DPR), each making measurements of ocean reflection at near-nadir incidence angles. Fig. 1 also provides the prediction for Ka-band and $\theta = 0^\circ$, showing that there is a change of nearly 14% over a range of SST from 0°C to 32°C . The variation with SST significantly exceeds that at Ku-band and is large enough that it could impact applications such as wind speed estimation using a Ka-band altimeter. For example, the sensitivity of σ_0 to wind speed found in the nominal AltiKa wind speed model function [7] suggests that such $\rho(\text{SST})$ variation translates to as much as 1.0-m/s error. This note uses these new satellite data to evaluate the ocean specular return ρ at Ka-band, compare results to that predicted by a seawater dielectric constant model, and discuss potential implications.

II. METHODS

In this letter, we attempt to isolate σ_0 variation due to the change in the specular reflectivity using large global ocean satellite radar data sets. We develop results using nadir or near-nadir incidence at Ka-band and also at the lower frequency C- and Ku-bands to allow comparison to the dielectric model and to provide a relative multifrequency assessment.

SARAL (Satellite with ARGos and ALtiKa) AltiKa radar altimeter data for the study come from the AVISO (<http://aviso.altimetry.fr>) Geophysical Data Record (GDR) products as contained in the Radar Altimeter Database System (RADS, <http://rads.tudelft.nl>). The radar center frequency is 35.75 GHz, and the nominal incidence angle is 0.0° . We use standard ocean data filtering and 10 cycles of global AltiKa data that extend from 65°S to 65°N in latitude and cover the time period of March 2013 to February 2014, a total of more than 58 300 measurements. The NRCS data from AltiKa have been corrected for atmospheric attenuation due to water vapor and cloud liquid water, and we allow all otherwise valid measurements that are not flagged for rain effects into the initial data set. Coincident 10-m ocean surface wind speed estimates come from ECMWF NWP analysis (6 hourly, 0.5° spatial resolution), while the SST is from the daily 0.25° NOAA high-resolution OI SST (version 2).

Global C- and Ku-band NRCS data at nadir incidence were also obtained from the 1-Hz Jason-2 ocean altimeter data set obtained from AVISO GDR products for this ocean altimeter mission. The radar center frequencies are 5.3 and 13.6 GHz, and the nominal incidence angle is 0.0° . We use standard data filtering approaches and 36 cycles of Jason-2 that extend from 60°S to $+60^\circ\text{N}$ and for the time period of May 2009 to June 2010, a total of 700 000 measurements. Flagging and atmospheric attenuation corrections to NRCS are performed in a manner similar to that using AltiKa, and the ancillary wind and SST come from the same sources.

GPM DPR σ_0 values come from version L2A-Ku and L2A-Ka data sets obtained via the NASA Precipitation Mission data server (<http://pmm.nasa.gov>). Selected data cover the period from April 1 to September 30, 2014, the latitude band of 60°S to 60°N , and include more than 180 000 measurements. The center frequencies at Ka- and Ku-band are 35.55 and 13.60 GHz. For this study, we evaluate data at both nadir

($\theta < 0.5^\circ$) and off-nadir ($\theta = 9^\circ \pm 0.1^\circ$). The second angle is included in the analysis because of known wind-wave insensitivity near $\theta = 10^\circ$. DPR data are filtered to exclude rain-impacted data and otherwise invalid operating conditions. Coincident surface wind and SST estimates come from the ECMWF surface analysis product (3 hourly, 0.125° resolution). The slightly broader surface footprint and high transmit power of DPR permit somewhat improved signal-to-noise in rain-free ocean NRCS measurements when compared to the ocean altimeters.

Models for the dependence of microwave emission and reflection on variation in the dielectric properties of seawater have been developed using several approaches [4]–[6]. We choose to compare observations to results from [6] in that this model has been developed specifically to encompass frequencies that extend below and above 36 GHz and a range of SST that extend from 2°C to 29°C . It also makes use of long-term satellite ocean radiometer measurements tied to estimation of the flat surface emissivity ($e = 1 - \rho$).

Two methods are taken to isolate σ_0 variation due to ρ with SST in (1). For AltiKa and Jason-2 data, we take the approach to assume that m_{seff} is closely related to wind speed [8], and it will be nearly fixed in value for a fixed wind speed. This should be particularly valid for a light-to-moderate wind speed of $U = 5$ m/s, where wave breaking impacts are limited and remaining nonwind variation in m_{seff} should mostly be tied to long wave (swell) variability [9]. If this impact is largely uncorrelated with ρ variation, then isolation of the term should occur. Note that we do not attempt to assess the absolute value of ρ in this note, due in large part to the requirement of an exacting absolute calibration of the satellite radar σ_0 . This calibration is typically only possible to within 1 dB. We can, however, adjust σ_0 with a single bias or offset α_{cal} for each radar and then assess ρ within (1). In this case, at angles near to nadir incidence and wind of 5 m/s, one finds

$$\rho_x(\text{SST}) = \sigma_0(\theta) \cdot m_{\text{seff}5} \cdot \alpha_{\text{cal}x} \quad (2)$$

where x is the radar frequency. For this study, we assume that $m_{\text{seff}5} = 0.032$ at $U = 5$ m/s following [9]. The values of α_{cal} are 1.05 for AltiKa and 1.19 and 0.57, respectively, for the Ku- and C-band channels of Jason-2.

Specific additional filtering of AltiKa and Jason-2 data was performed during this process to limit apparent noise in the estimation for the coldest and warmest waters. For SST below 5°C , data were limited to a significant wave height between 1 and 4 m, where this was viewed as a proxy outlier filter for sea ice and events with large swell fields that may impact σ_0 . For SST greater than 25°C , data were limited to cases with columnar atmospheric water vapor below 40 mm and $8 < \sigma_0 < 16$ dB, the former to limit impact of erroneous atmospheric corrections under high humidity and the latter to filter outliers tied to known slick surface conditions in the tropics.

For GPM, we take the same approach to derive results at nadir and do so for both Ku- and Ka-band at $\theta < 1^\circ$. Because the GPM DPR also scans across swath in θ , a second result is also derived for $\theta = 9^\circ$. NRCS measurements near this angle are known to be nearly invariant with ocean roughness variation

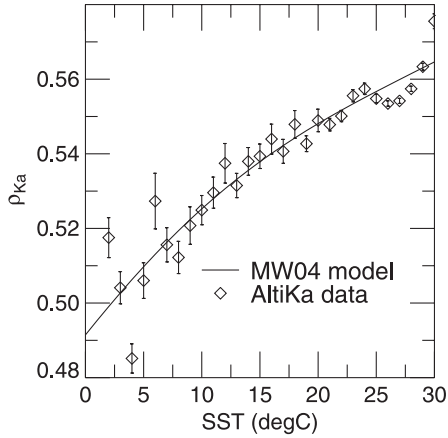


Fig. 2. Variation of ρ_{Ka} with seawater temperature change as predicted by MW04 (solid line) and observed using global AltiKa radar altimeter data for the case of $U = 5 \text{ ms}^{-1}$ and $m_{\text{seff}} = 0.032$ as discussed in the text. Error bars represent 99% confidence intervals.

[1], [10], [11], and thus, one may observe near isolation of ρ for all m_{seff} . This negates the need to limit results to a wind speed of 5 m/s. In this latter case, (2) is still relevant, and one simply needs the mean value of $m_{\text{seff}5}$ and a factor α_{cal} derived for $\theta = 9^\circ$. The values of α_{cal} for GPM at Ka-band and $\theta = 0$ and 9° are 1.00 and 2.31, and at Ku-band, they are 1.02 and 2.48.

III. RESULTS

The results from the global bin averaging of ocean AltiKa σ_0 data versus SST following (2) are shown in Fig. 2 along with the Ka-band prediction from [6]. It is clear that the data are in close agreement with the model for the entire range of SST, and the worst case differences occur toward SST below 6 °C. In general, the differences are on the order of 0.02 in magnitude, well below 0.5%, and often statistically equivalent to the model based on the estimated confidence limits. No apparent trends away from the model at any specific temperature are evident. As noted previously, the AltiKa data were filtered to attempt to exclude sea ice at low SST, but at both low and high SSTs, smooth surface returns are often encountered and difficult to filter from the data. These outliers can impact the bin average mean as well as the computed error bars that presume Gaussian noise in the sample population.

Multifrequency results are provided in Fig. 3. In this case, the data are provided after normalization to the average result at $\text{SST} = 18^\circ\text{C}$. At Ka-band, the results from AltiKa and GPM are quite self-consistent and in agreement with the model's prediction. The data show a range of variation that covers nearly 10% from 5 °C to 25 °C and that the radar results generally fall within $\pm 0.5\%$ of the model. A similar agreement with model and between sensors is observed at Ku-band, with the most obvious difference being the more limited expected and observed variation with SST. The Ku-band model predicts a slight but perceptible drop off below 10 °C. The satellite data, even with their apparent or inherent noise, do appear to provide confirmation of this decrease. Results at C-band are in agreement with the model to $\pm 1\%$ over all ocean temperatures, with the model predicting almost no variation with SST. The

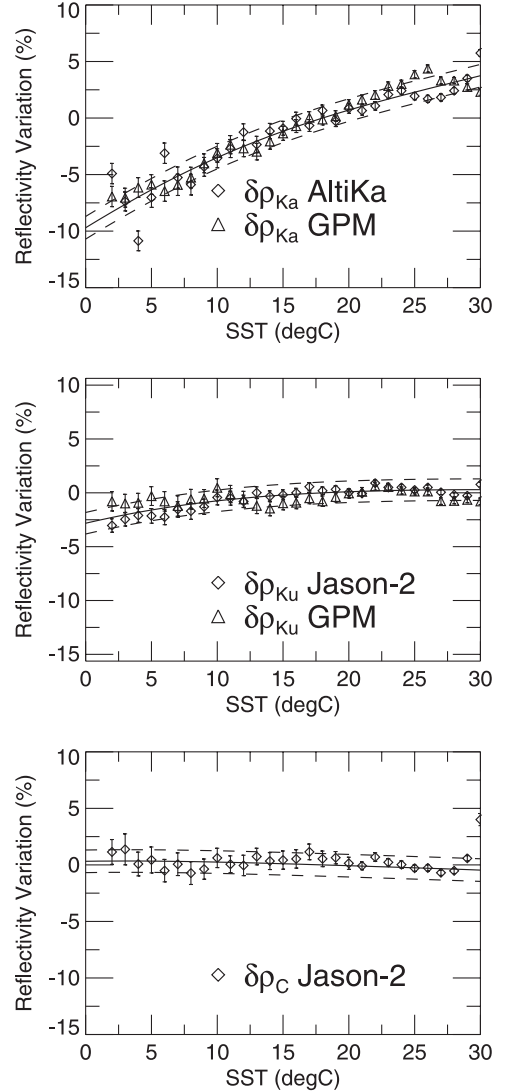


Fig. 3. Variation of ρ (in percent) with seawater temperature change as predicted by MW04 and as measured by the noted satellites. Results are provided at Ka-, Ku-, and C-band. In each case, the data are normalized by their value at $\text{SST} = 18^\circ\text{C}$. The dashed lines represent $\pm 1\%$, and the error bars represent 99% confidence intervals.

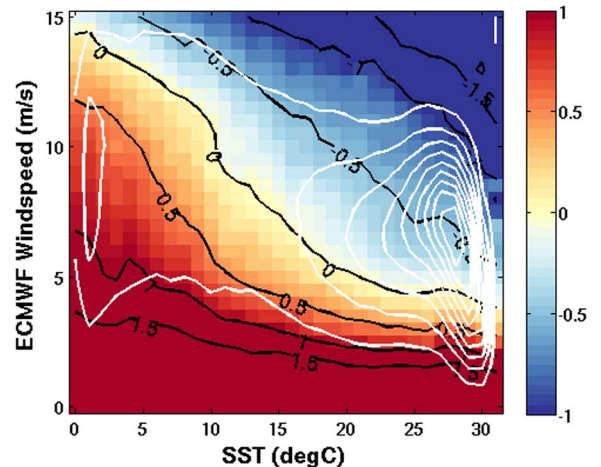


Fig. 4. Observed difference between AltiKa and ECMWF wind speed estimates (colorbar) as a function of SST and ECMWF wind speed. The white contours are the relative data population, and the black contours are for the wind difference at 0.5-m/s intervals. Results are averaged over the full data period of 18 months.

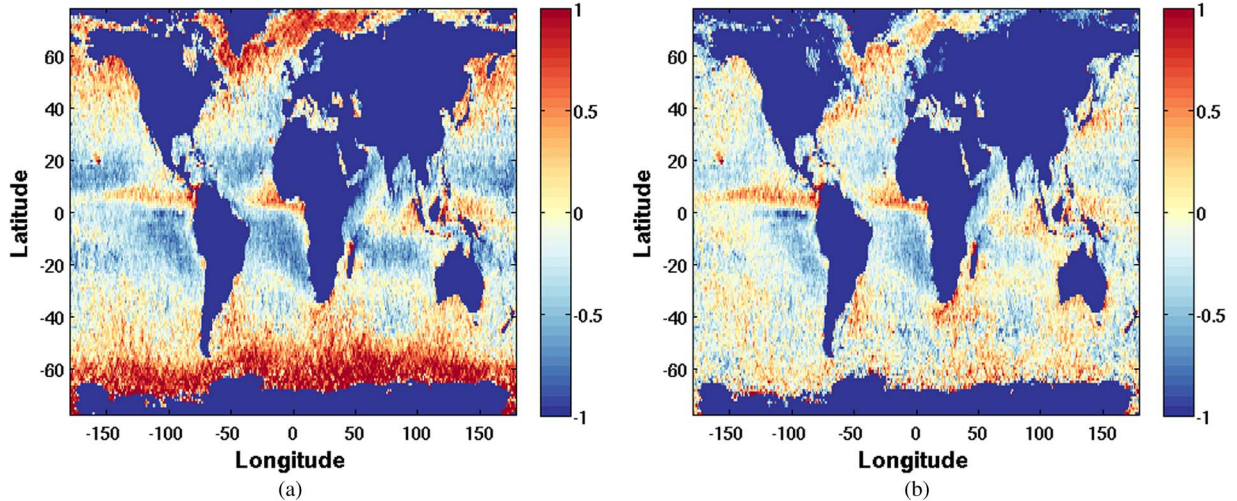


Fig. 5. Global map of the average surface ocean wind speed difference between the AltiKa and ECMWF estimates for 18 months of AltiKa measurements. The panel at the left shows the result obtained using the standard AltiKa GDR wind speed derived from σ_0 . The second panel provides the difference after applying a point-by-point σ_0 correction for SST-dependent reflectivity variation as discussed in the text prior to application in the wind speed algorithm. (a) AltiKa-ECMWF. (b) After AltiKa correction.

C-band altimeter of Jason-2 is not optimized for precise σ_0 measurements, and thus, more noise and variability are not unexpected in these data. The same analysis was performed at C- and Ku-band using a year of Jason-1 altimeter data (not shown) with nearly identical results.

All-wind condition GPM data at $\theta = 9^\circ$ were also evaluated and yielded results (not shown) that are nearly equivalent to the Ku- and Ka-band GPM results in Fig. 3. The one observed exception is that the off-nadir GPM Ka band data tended to overestimate ρ slightly more than GPM in Fig. 3 for SST above 25°C . We attribute this to possible limitations in our data prefiltering and use of all wind speeds and, alternatively, to potential SST-dependent bias in the atmospheric corrections applied to the GPM σ_0 data for this longer path length and warm moist atmospheres at high SST.

IV. DISCUSSION AND CONCLUSIONS

Satellite radar ocean backscatter data at Ka-band show close agreement between predicted and observed estimates of the Fresnel reflection coefficient variation with SST. Our result is congruent in its SST variation with [6] and shows that near-nadir ocean σ_0 at 36 GHz varies by nearly 15% between the coldest and warmest ocean temperatures. We affirm that this level of variation is much greater than what is observed and predicted at C- and Ku-band, the more common satellite ocean radar transmit frequencies. Results were derived for the case where wind speed was limited to cases near 5 m/s.

There are several potential implications tied to these findings.

This type of variation is not yet carried in satellite ocean surface backscatter applications and analyses using, for example, AltiKa [7] or the GPM DPR. It may also be relevant to CloudSat W-band analyses [13]. While the temperature dependence may be small, studies directed at inferring sea surface roughness properties may be compromised by issues such as spurious correlation that is expected due to the zonal covariance between ocean wind-waves and SST properties such as Southern Ocean

swell and low SST. SST impact may also have potential ramifications for the GPM rain radar surface reflectance technique [11] that relies on the assumption of near invariance in the surface backscatter near θ of 10° and between Ku- and Ka-band frequencies.

With respect to applications, any derivation of surface wind speed from uncorrected σ_0 may carry an SST-dependent error. To assess this, one can compare the wind speed data derived from AltiKa NRCS data using [7] to the ECMWF surface wind estimates as shown in Fig. 4. Looking near the median ocean wind speed of 7 m/s, one sees a nearly linear SST-dependent bias in the annual averaged data, indicating overestimation in cold water, overestimation for very warm SST, and near 0 bias at SST of about 19°C . Point-by-point correction using coincident SST estimates could yield a simple first-order correction, analogous to the use of a flat surface emissivity term used in radiometer applications. One method to apply such a correction to the AltiKa wind speed data can be approached by adjusting each σ_0 measurement for reflectivity variation based on a scaling factor β , defined as $\rho(\text{SST})/\rho(\text{SST}_{\text{ref}})$. The denominator $\rho(\text{SST}_{\text{ref}})$ is a function of σ_0 and is ρ at the ocean temperature observed for the case where the globally averaged wind speed difference between the reference ECMWF wind and ALtiKa GDR wind speed estimates is 0. As inferred from Fig. 4, this reference temperature decreases with σ_0 (or as the wind speed increases). The results of such an *ad hoc* correction, with ρ derived using [6], are shown in Fig. 5 for a global averaging over all wind speeds and the 18-month period from March 2014 to August 2015. There is obvious reduction in the wind speed bias that is especially evident in colder water. A fuller accounting for this likely error in AltiKa winds is left to future studies. Future work combining more exacting analyses of passive and active data at Ka-band may also lead to slight refinement of the temperature-dependent dielectric model [6].

These SST-dependent radar backscatter results at Ka-band are expected for both near- and off-nadir angles. For instance, at $\theta = 50^\circ$, the impact will be greater than observed at nadir

for vertical polarization and slightly less for horizontal. Thus, proposed new Ka-band ocean systems for wide-swath altimetry [2] and Doppler ocean wind vector scatterometry may need to consider this phenomena within future algorithm design.

ACKNOWLEDGMENT

The authors would like to thank T. Meissner for providing the programs needed to implement the seawater permittivity model.

REFERENCES

- [1] F. C. Jackson, W. T. Walton, D. E. Hines, B. A. Walter, and C. Y. Peng, "Sea surface mean square slope from Ku-band backscatter data," *J. Geophys. Res.*, vol. 97, no. C7, pp. 11 411–11 427, Jul. 1992.
- [2] M. Durand *et al.*, "The Surface Water and Ocean Topography mission: Observing terrestrial surface water and oceanic submesoscale eddies," *Proc. IEEE*, vol. 98, no. 5, pp. 766–779, May 2010.
- [3] J. Verron *et al.*, "The SARAL/AltiKa altimetry satellite mission," *Marine Geodesy*, vol. 38, pp. 2–21, Jan. 2015.
- [4] L. A. Klein and C. T. Swift, "An improved model for the dielectric constant of sea water at microwave frequencies," *IEEE Trans. Antennas Propag.*, vol. 25, no. 1, pp. 104–111, Jan. 1977.
- [5] W. Ellison *et al.*, "New permittivity measurements of seawater," *Radio Sci.*, vol. 33, no. 3, pp. 639–648, May/Jun. 1998.
- [6] T. Meissner and F. Wentz, "The complex dielectric constant of pure and sea water from microwave satellite observations," *IEEE Trans. Geosci. Remote Sens.*, vol. 42, no. 9, pp. 1836–1849, Sep. 2004.
- [7] J. Lillbridge, R. Scharroo, S. Abdalla, and D. Vandemark, "One and two parameter wind speed models for Ka-band altimetry," *J. Atmos. Ocean. Technol.*, vol. 31, no. 3, pp. 630–638, Mar. 2014.
- [8] C. Cox and W. Munk, "Slopes of the sea surface deduced from photographs of sun glitter," *Bull. Scripps Inst. Oceanogr.*, vol. 6, no. 9, pp. 401–488, 1956.
- [9] D. Vandemark, B. Chapron, J. Sun, G. H. Crescenti, and H. C. Graber, "Ocean wave slope observations using radar backscatter and laser altimeters," *J. Phys. Oceanogr.*, vol. 34, no. 12, pp. 2825–2842, Dec. 2004.
- [10] N. Tran, B. Chapron, and D. Vandemark, "The effect of long waves on Ku-band backscatter at low incidence angles using TRMM and altimeter data," *IEEE Geosci. Remote Sens. Lett.*, vol. 4, no. 4, pp. 524–546, Oct. 2007.
- [11] R. Meneghini, L. Liao, S. Tanelli, and S. L. Durden, "Assessment of the performance of a dual-frequency surface reference technique over ocean," *IEEE Trans. Geosci. Remote Sens.*, vol. 50, no. 8, pp. 2968–2977, Aug. 2012.
- [12] N. Majurec, J. T. Johnson, S. Tanelli, and S. L. Durden, "Comparison of model predictions with measurements of Ku- and Ka-band near-nadir normalized radar cross sections of the sea surface from the genesis and rapid intensification processes experiment," *IEEE Trans. Geosci. Remote Sens.*, vol. 52, no. 9, pp. 5320–5332, Sep. 2014.
- [13] S. L. Durden, S. Tanelli, and G. Dobrowalski, "CloudSat W-band radar measurements of surface backscatter," *IEEE Geosci. Remote Sens. Lett.*, vol. 8, no. 3, pp. 401–405, May 2011.